NASA TECHNICAL MEMORANDUM

UB
NASA TM X-2111

INVESTIGATION OF FLOW CHARACTERISTICS OF SOME WIRE-FORM AND LAMINATE-FORM POROUS MATERIALS

by Albert Kaufman and Hadley T. Richards

Lewis Research Center
Cleveland, Ohio 44135

NATIONAL AERONAUTICS AND SPACE ADMINISTRATION • WASHINGTON, D. C. • OCTOBER 1970

[redacted]

[redacted]

1. Report No.	2. Government Accession No.	3. Recipient's Catalog No.
NASA TM X-2111		

4. Title and Subtitle	5. Report Date
INVESTIGATION OF FLOW CHARACTERISTICS OF SOME WIRE-FORM AND LAMINATE-FORM POROUS MATERIALS (U)	October 1970
	6. Performing Organization Code
7. Author(s)	8. Performing Organization Report No.
Albert Kaufman and Hadley T. Richards	E-5748
	10. Work Unit No.
9. Performing Organization Name and Address	720-03
Lewis Research Center National Aeronautics and Space Administration Cleveland, Ohio 44135	11. Contract or Grant No.
	13. Type of Report and Period Covered
12. Sponsoring Agency Name and Address	Technical Memorandum
National Aeronautics and Space Administration Washington, D.C. 20546	14. Sponsoring Agency Code

15. Supplementary Notes

16. Abstract

Experimentally determined flow characteristics were correlated with standard flow rates and absolute filtration ratings of wire-form materials and with functions of hydraulic diameters and external hole spacings of laminate-form materials. Effects on flow characteristics of specimen curvature and use of high temperature air up to 840° F (722 K) were investigated. The conclusion was drawn that flow rates both for elevated temperature conditions and for specimen curvatures simulating leading-edge radii of turbine blades can be predicted with good accuracy from correlations developed herein and the basic flow equation for porous media.

17. Key Words (Suggested by Author(s))	18. Distribution Statement
Transpiration cooling Turbine blades Fluid flow	[redacted]

19. Security Classif. (of this report)	20. Security Classif. (of this page)	21. No. of Pages	22. Price
[redacted]	Unclassified	23	

GROUP 4
Downgraded at 3 year intervals;
declassified after 12 years

[redacted]

*For sale by the Clearinghouse for Federal Scientific and Technical Information
Springfield, Virginia 22151

[redacted]

INVESTIGATION OF FLOW CHARACTERISTICS OF SOME WIRE-FORM AND LAMINATE-FORM POROUS MATERIALS*

by Albert Kaufman and Hadley T. Richards

Lewis Research Center

SUMMARY

In order to be able to predict flow rates under any combination of design conditions a study was made to determine relations between flow characteristics and geometrical parameters of wire-form and laminate-form porous materials suitable for transpiration cooling of turbine blades for advanced airbreathing engines. Effects on the flow rates of airflow temperatures from 70° to 840° F (294 to 722 K) were investigated for permeability-coefficient-to-thickness ratios from 10×10^{-10} to 20×10^{-10} foot (3.0×10^{-10} to 6.1×10^{-10} m) for the wire-form materials, and from 8×10^{-10} to 60×10^{-10} foot (2.4×10^{-10} to 18.2×10^{-10} m) for the laminate materials. In addition, the effect of curvature of the wire-form sheets was studied for a range of radii from 0.5 to 0.1 inch (1.27 to 0.25 cm). Flow characteristics obtained from cold flow tests conducted in the present investigation and by other investigators were found to correlate well with the standard flow rates and absolute filtration ratings for the wire-form materials and with a parameter combining hydraulic diameter and hole spacing for the laminate-form materials. In general, the effects of differences in air temperature and specimen curvature on the flow rates were found to be minor. Flow rates under these conditions could be predicted with good accuracy from the flow characteristic correlations and the basic flow equation for porous media.

INTRODUCTION

It was the basic purpose of this study to determine if unique relations could be discovered among the terms used to define the flow characteristics of porous material that

*Title unclassified.

would permit the calculation of flow rates through the walls of transpiration-cooled turbine blades for any design condition. Without such relations, it would be necessary to resort to extensive experimental flow tests since there are too many unknowns in the applicable flow equation to allow a direct analytical solution.

The standard equation that has been used for calculating the flow rate through the porous walls of transpiration-cooled structures is the so-called "Green equation" which was suggested in reference 1 and is shown by equation (1):

$$\frac{\left(P_1^2 - P_2^2\right)g_c}{\tau\mu^2(2RT)} = \alpha\left(\frac{G}{\mu}\right) + \beta\left(\frac{G}{\mu}\right)^2 \tag{1}$$

(The symbols in this report are defined in the appendix.) For the sake of brevity, the mass airflow rate per unit surface area G will henceforth simply be called flow rate. In equation (1) the flow rate can be calculated for a particular combination of fluid temperature and pressures across the porous wall with a knowledge of the flow coefficients α and β. The α coefficient is a measure of the viscous shear losses and the β coefficient is a measure of the inertial losses through the tortuous coolant passages of the porous structure. Two other terms which have been used to characterize the flow capabilities of porous materials are G_s, which is an airflow rate under certain standard conditions given for the subscript s in the appendix, and K, which is a permeability coefficient defined by

$$K = \frac{2\tau T_s R\mu G_s}{\left(P_{1,s}^2 - P_{2,s}^2\right)g_c} \tag{2}$$

There is frequent confusion between porosity, which is the ratio of the void volume of the body to the total volume of the body, and permeability, which is a criterion of the capability of the material to allow passage of fluid through it. Porosity is not related to permeability in certain wire-form structures where many passages are discontinuous or dead-ended, as is discussed in reference 2.

In order to solve equation (1) for G if P_1, P_2, and T are known, or as is often the case, to solve it for P_1 if G, P_2, and T are known, it is necessary to find a unique relation among the variables. This relation may be between either α or β and either G_s or K or both α and β against some physical parameter of the material which is either known or measureable, such as porosity, filtration rating, hydraulic diameter, or hole spacing. It would be preferable to have a correlation with a physical parameter in order to make it easier to specify the porous configuration required for a particular design application.

A common method of fabricating porous materials for transpiration-cooled structures is to wind wire over a removable mandrel and then roll and sinter the wire wrapping to a desired permeability and thickness. Other transpiration-cooled structures have been constructed from sheet metal laminates by photoetching passages and holes in the laminates and diffusion bonding them together. The internal geometries of wire-form and laminate-form porous materials are described in more detail in references 2 and 3, respectively. Excellent correlation of flow data for air temperatures up to 300° F (422 K) using equation (1) was reported in reference 3 for both wire and laminate porous materials.

The purposes of this investigation are threefold: (1) to develop unique relations between flow characteristics and determinable physical characteristics of wound wire-form and laminate-form porous materials from cold flow tests; (2) to experimentally investigate the effects of airflow temperatures up to 840° F (722 K) on the flow characteristics of both materials; and (3) to investigate the effect of sheet curvature on flow through wire-form porous sheets for curvatures typical of those encountered in turbine blade airfoil shells.

In developing relations among the flow and physical characteristics, cold flow data from wire-form sheets for G_S ranges from 3.5×10^{-3} to 6.0×10^{-3} pound per second inch^2 (2.46 to 4.22 kg/sec-m^2) or K/τ ranges from 14×10^{-10} to 20×10^{-10} foot (4.3×10^{-10} to 6.1×10^{-10} m) were used in conjunction with cold flow data from reference 3 for both wire- and laminate-form sheets for G_S ranges from 0.2×10^{-3} to 20.0×10^{-3} pound per second inch^2 (0.14 to 14.1 kg/sec-m^2) or K/τ ranges from 0.7×10^{-10} to 30×10^{-10} foot (0.2×10^{-10} to 9.1×10^{-10} m). These flow rate and permeability ranges encompass the design requirements for transpiration-cooled blades in advanced airbreathing engines.

Effects of curvature of wire-form sheet specimens with radii from 0.1 to 0.5 inch (0.25 to 1.27 cm) and effects of fluid temperatures from 700° to 840° F (644 to 722 K) on both wire and laminate materials were investigated using a different group of specimens from that used in the correlation study. These latter specimens were also used to compare measured flow rates at maximum temperature or curvature conditions against flow rates predicted from equation (1) and the flow characteristic correlations.

EXPERIMENTAL APPARATUS AND PROCEDURE

Test Specimens

The dimensional, flow, and permeability specifications of all test specimens from which data were obtained are summarized in table I. Table I also includes specimens

TABLE I. - TEST SPECIMEN SPECIFICATIONS

Type of test	Source	Material	Specimen size		Standard flow rate, G_s		Permeability-coefficient-to-thickness ratio, $(K/\tau)\times10^{10}$	
			in.	cm	lb/sec-in.^{2}	kg/sec-m^2	ft	m
Flow data correlation	Present study	Wire-form	6 × 12 × 0.024	15.2 × 30.5 × 0.061	0.0035 to 0.006	2.46 to 4.22	14 to 20	4.3 to 6.1
Curvature effect		Wire-form	0.1 to 0.5 R × 2 × 0.024	0.25 to 1.27 R × 5.08 × 0.061	0.0035 to 0.006	2.46 to 4.22	14 to 20	4.3 to 6.1
Elevated temperature effect for 700° to 840° F (644 to 722 K) air		Wire-form	1.625 D × 0.025	4.128 D × 0.064	0.003 to 0.006	2.11 to 4.22	10 to 20	3.0 to 6.1
		Laminate-form	1.625 D × 0.024	4.128 D × 0.061	0.0026 to 0.020	1.83 to 14.1	8 to 60	2.4 to 18.2
Flow data correlation	Reference 3	Wire-form	1.132 D	2.875 D	0.0002 to 0.006	0.14 to 4.22	0.7 to 22	0.2 to 6.7
		Laminate-form	1.132 D	2.875 D	0.0004 to 0.020	0.28 to 14.1	1 to 30	0.3 to 9.1
Elevated temperature effect for 300° F (422 K) air		Wire-form	1.132 D	2.875 D	0.0018 to 0.003	1.26 to 2.11	7 to 11	2.1 to 3.4
		Laminate-form	1.132 D	2.875 D	0.002 to 0.003	1.41 to 2.11	9 to 10	2.7 to 3.0

tested in reference 3. The variation in flow characteristics in wire-form porous materials using room-temperature air was investigated over seven rectangular sheets approximately 6 by 12 inches (15.2 by 30.5 cm) and 0.024 inch (0.061 cm) thick. The sheet specimens were fabricated to a standard flow rate range from 3.5×10^{-3} to 6.0×10^{-3} pound per second-inch^2 (2.46 to 4.22 kg/sec-m^2). These specimens were used to study the variation in α, β, and G_s at different locations on the surfaces. The average α, β, and G_s values from each of these seven sheets were used to correlate the flow characteristics against each other and against physical parameters. A sheet specimen is shown mounted in a test fixture in figure 1.

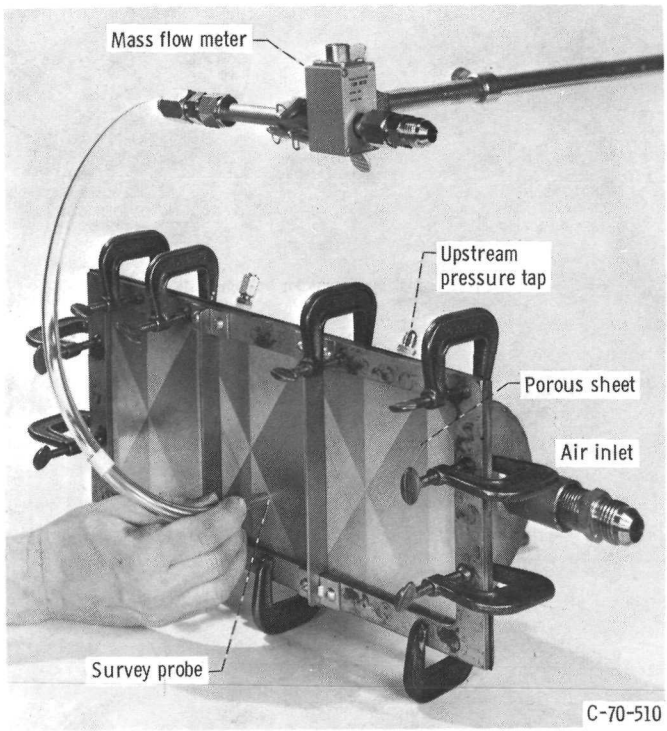

Figure 1. - Wire-form porous sheet in flow test fixture.

Isothermal flow tests using 70° to 840° F (294 to 722 K) air were conducted on three disk specimens of laminate-form materials and two disk specimens of wire-form materials. These specimens had overall diameters of 1.625 inches (4.128 cm) and flow diameters of 1.375 inches (3.492 cm). These disks were cut from material supplied by Allison Division of General Motors for all three permeability levels tested in reference 3. However, it was found that, due to the radiation losses from the test section, only with the high-flow-level specimens could the air heater supply significantly higher

temperature air at the test section than the 300° F (422 K) air used in reference 3. The high-flow-level specimens had flow rates from 3.0×10^{-3} to 6.0×10^{-3} pound per second-inch^2 (2.11 to 4.22 kg/sec-m^2) for the wire-form material and 2.6×10^{-3} to 20.0×10^{-3} pound per second-inch^2 (1.83 to 14.1 kg/sec-m^2) for the laminate-form material under the standard conditions of temperature and pressure described in the appendix. Typical laminate- and wire-form disk specimens are shown in figure 2.

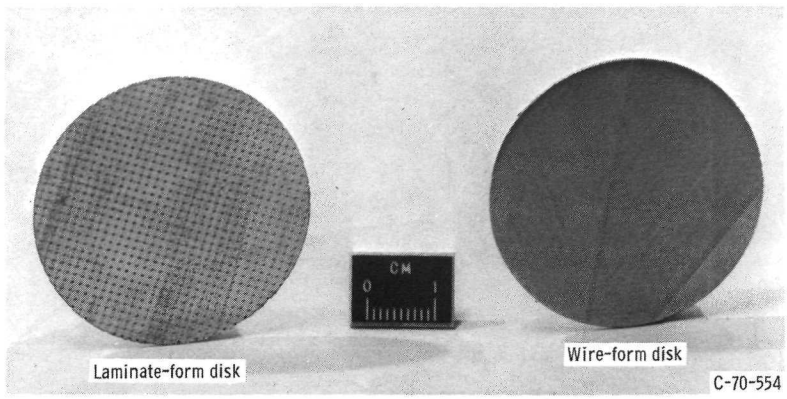

Figure 2. - Disk specimens for hot flow tests.

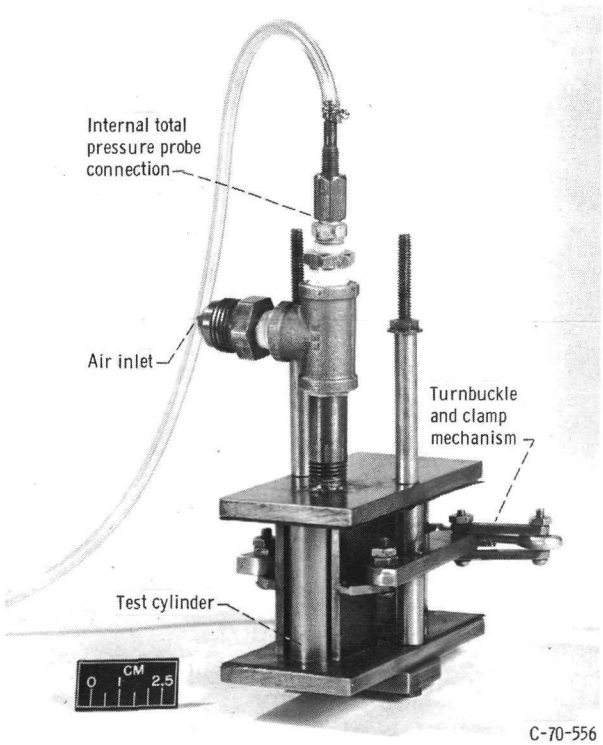

Figure 3. - Curved specimen in test fixture.

Three specimens were cut from wire-form sheets and seam-welded longitudinally to form cylinders with initial radii of 0.5 inch (1.27 cm). These specimens were subsequently compressed diametrally as shown in figure 3 to form a number of curved shapes simulating turbine blade leading-edge radii from 0.5 to 0.1 inch (1.27 to 0.25 cm).

Flow Test Apparatus

The test setup consisted of an air supply system and three test fixtures for the flat sheet, curved, and disk specimens (fig. 4).

Air supply system. - A schematic diagram of the basic air supply system with the associated instrumentation is shown in figure 4. Air at 125 psig (86.2 N/cm^2) was supplied through a dryer and filter, two pressure regulators in series, an electric air

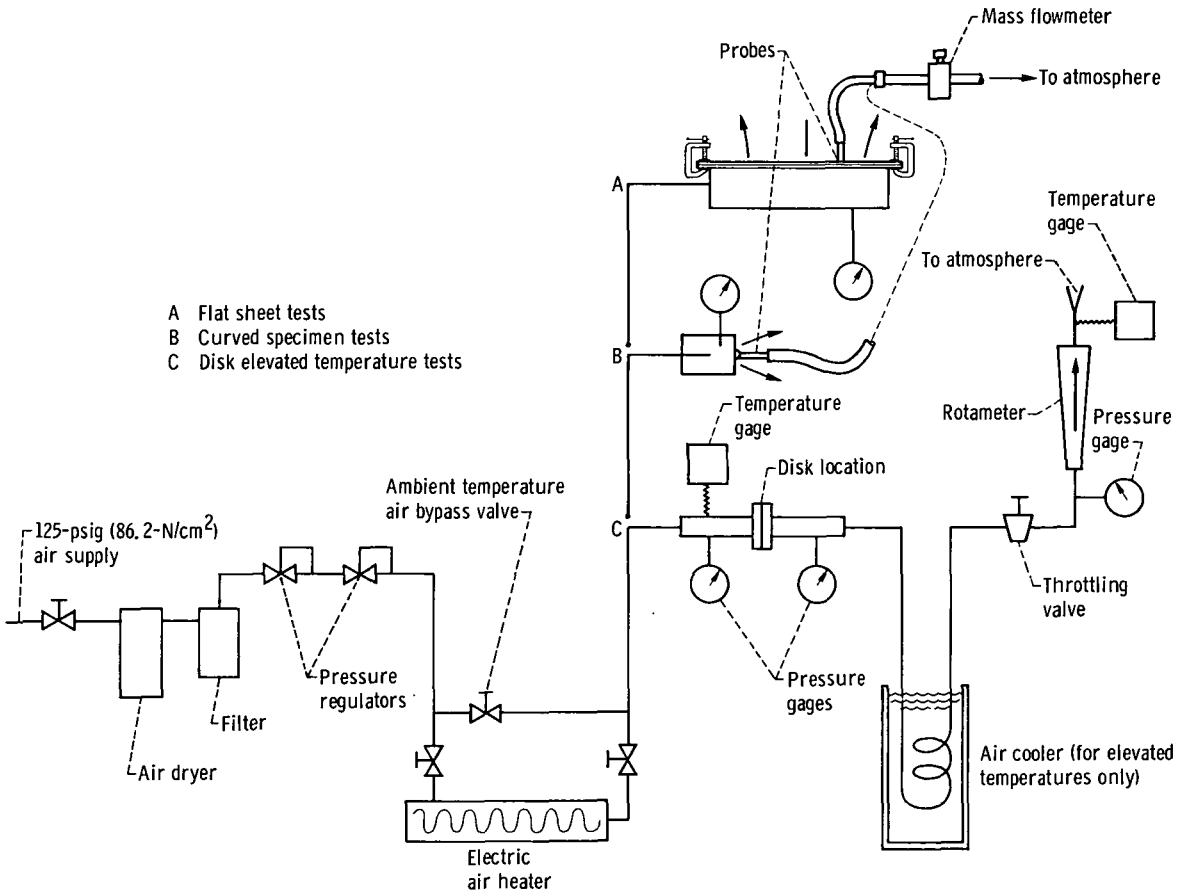

Figure 4. - Porous material flow setup.

heater capable of heating air to 1000° F (811 K) with a bypass for ambient temperature tests, and into the test section. When the air heater was used, the heated air flowing through the porous surface was collected, ducted through a cooler, and passed through a throttling valve and a rotameter before exhausting to the atmosphere.

Local airflow through the porous surface during a room temperature test was conducted through a probe made from acrylic plastic tubing and measured in a calibrated mass flowmeter. This flowmeter consisted of a commercially available hot-wire anemometer in a venturi with an electrical network to permit linearized mass flow readings. The surface of each probe was formed to the contour of the porous sheet at the measurement location. The flowmeter had a very low pressure drop which minimized leakage around the rim of the probe. A representative probe and the mass flowmeter are shown in figure 1.

The pressure differences and levels across the test section were controlled by the pressure regulators for the flat specimens and wire-form curved specimens. For the elevated temperature tests on the disk specimens, the downstream pressure was set with the exhaust throttling valve. Downstream and upstream pressures were measured on calibrated bellows-actuated pressure gages with a maximum pressure of 50 psia (34.5 N/cm^2) and an accuracy of ±0.1 percent of full scale. The air temperature at the porous surface was measured with a copper-constantan thermocouple probe.

Flat sheet specimen installation. - The flat wire-form porous sheets were clamped and sealed to the flange of the test fixture shown in figure 1 against a flat 0.063-inch (0.160-cm) thick neoprene gasket. The test fixture clamping frame had two transverse webs to prevent excessive deflection of the test specimen.

Disk specimen installation. - The disk specimens were clamped between copper gaskets which sealed them upstream, downstream, and around the outer rims to confine any leakage from the porous edges. The exterior surface of the test fixture was insulated with glass wool to minimize heat losses and to ensure that a constant disk temperature was maintained.

Curved specimen installation. - Initially cylindrical specimens were mounted in the clamp-type holder shown in figure 3. The projecting curved segment of the specimen was deformed to a new radius by increasing the clamping pressure through a turnbuckle and linkages which moved like a scissors. Probes were formed to the surface contour for each of the new test radii. The surface areas of the probes were determined mathematically after first viewing each shaped probe in an optical comparator to determine the radius of curvature and then measuring the internal diameter to the nearest 0.001 inch (0.0025 cm). This information was combined in a mathematical expression defining the area of the intersection of the probe and the curved surface.

Testing Procedure

Flow tests were conducted on each porous specimen for from four to 10 different combinations of upstream and downstream pressures. The air temperatures were measured in the upstream plenum of the test fixture for the disk tests and at the downstream surface for the other tests. All testing for the flat sheet and curved specimens was done by increasing the upstream supply pressure in steps to a reasonable maximum pressure at which the specimens started to bulge with barometric downstream pressure. At each step, the local airflow, as sampled by the probe, was measured at 36 locations over the 6 by 12 inch (15.2 by 30.5 cm) flat sheet specimens and at three longitudinal locations (near the bottom and top and at the center) of the curved specimens for each bend radius. In the case of the disk specimens, the upstream pressure was maintained constant while the downstream pressure was increased in steps. The total flow passing through the 1.375-inch (3.492-cm) diameter test section was measured under isothermal conditions with the highest temperature air that could be flowed through the porous specimen.

ANALYTICAL PROCEDURE

The airflow rates through the porous materials were correlated on the basis of the Green equation (eq. (1)). This equation can be rewritten as

$$\frac{\left(P_1^2 - P_2^2\right)g_c}{\tau\mu\,(2RTG)} = \alpha + \beta\left(\frac{G}{\mu}\right) \tag{3}$$

wherein β is an inertial resistance coefficient defining losses through the tortuous coolant passages and α is a viscous resistance coefficient defining the viscous shear losses. At low velocities, α is also equivalent to the reciprocal of the permeability coefficient of the material.

The resistance coefficients were obtained from equation (3) by plotting flow data over a range of pressure drops across the porous specimens in terms of the parameter $\left(P_1^2 - P_2^2\right)g_c/\tau\mu(2RTG)$ as a function of G/μ. The coefficients α and β were the intercepts and slopes, respectively, of the resulting staright lines.

The α and β terms were determined for each wire- and laminate-form porous disk and for each location on the wire-form porous sheet and curved specimens by taking measurements of flow rate at four to 10 different combinations of inlet and discharge pressures. The data were then entered into computer program which plotted

$(P_1^2 - P_2^2)g_c/\tau\mu(2RTG)$ against G/μ, computed the best straight line through the plotted points by means of the method of least-mean-squares, checked the linearity of the data, determined the α and β coefficients, and calculated the flow rate G_s.

The average α and β coefficients from each porous specimen over the 36 locations in each flat sheet were then correlated with G_s and various parameters of the materials which could be used to define the physical structure. Data from reference 3 were also used for these correlations. Among the physical parameters investigated were porosity, filtration rating, hydraulic diameter, and mean diameter. The wire-form material flow characteristics were found to correlate best with the absolute filtration rating (AFR) as determined from a limited number of bead tests conducted by the Bendix Corporation and reported in reference 4. There is a linear relation between G_s and the absolute filtration rating of the material, as shown in figure 5 which based on a similar figure in reference 4. The absolute filtration rating is equivalent to the diameter of the largest bead out of a slurry containing glass beads of known diameters which

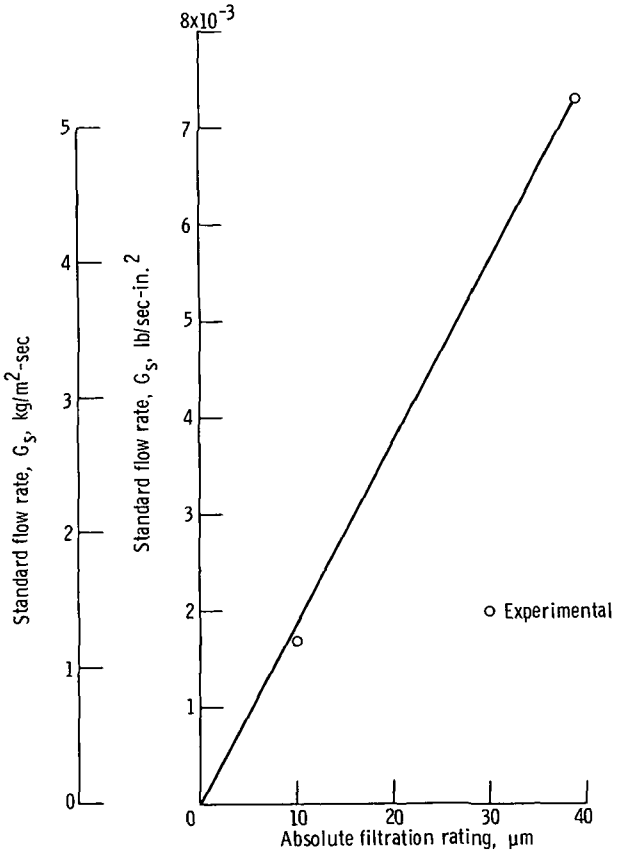

Figure 5. - Airflow rate - filtration rating relation for wound wire-form porous sheet, based on Bendix bead tests. (Based on similar figure in ref. 4.)

flows through the porous material. The sheet specimens were not tested directly since the glass bead test is destructive and the porous sheets were required for other applications. However, the relation shown in figure 5 can be used in computing the absolute filtration rating from the G_s values for all the wire-form porous specimens, including those for which flow test results were reported in reference 3. The best α and β correlation among the parameters investigated for the laminate-form material was obtained using a function consisting of the hydraulic diameter at the minimum constriction and the exit hole spacing. Only correlations with these parameters for each material type will be discussed.

RESULTS AND DISCUSSION

Variations of Flow Characteristics of Wire-Form Sheets

Results of airflow measurements at 36 locations on each of seven wire-form porous sheets are summarized in table II in terms of the variations in the flow characteristics α, β, and G_s from their average values over the sheets. The worst overall deviation in flow characteristics occurred in sheet 3. For this sheet the α deviation ranged from +86.0 percent to -39.2 percent from the average of the sheet. Similarly, the β variation was from +64.5 percent to -42.5 percent of the sheet average. Although the fluctuations in the resistance coefficients appear large, the flow rates for the standard

TABLE II. - VARIATION OF FLOW CHARACTERISTICS OVER HIGH-PERMEABILITY WIRE-FORMED SHEETS

Sheet number	Variation from average value over a sheet, based on measurements at 36 locations in sheet, percent					
	Viscous resistance coefficient, α		Inertial resistance coefficient, β		Flow rate, G_s	
	+	-	+	-	+	-
1	43.1	16.9	73.8	29.1	10.3	14.7
2	35.3	29.0	19.7	25.3	10.2	10.5
3	86.0	39.2	64.5	42.5	10.3	11.0
4	21.0	36.3	23.7	17.6	8.3	9.6
5	28.0	19.7	13.3	19.4	9.4	7.8
6	26.4	21.1	32.8	21.9	8.3	14.1
7	28.9	27.9	63.6	26.1	8.0	16.3

conditions were relatively insensitive to these changes, as can be seen by the fact that the variation in G_s in sheet 3 was within 11.0 percent of the average. The reason for the insensitivity of the G_s values to variations in the resistance coefficients was that when α was large, β tended to be small and conversely when α was small, β tended to be large. Also, from an inspection of equation (1) it is seen that as the flow rates become very small they will be increasingly affected by an inaccuracy or variation in α and as they become very large they will be influenced more by fluctuations in β. In general, the local flow rates at any location in the sheets were within ±11 percent of the average for the sheet although there were a few instances where the variations were as much as 15 or 16 percent.

Wire-Form Material Flow Correlation

The average viscous and inertial resistance coefficients from both the present investigation and reference 3 wire-form porous sheet flow results are presented in figure 6 as logarithmic functions of the average G_s of each specimen. These data generally follow straight lines on the log-log plots of figures 6(a) and (b) except for some of the high-permeability-level sheet data (ref. 3) in figure 6(a). Some of the α values from reference 3 which could not be plotted in figure 6 were negative, which is a physical impossibility. However, NASA-Lewis data for similar permeability level specimens did not demonstrate the sharp drop in α shown by the data from reference 3. The reason for the discrepancy in figure 6(a) between the α values of NASA and those of reference 3 is unknown. From figure 6 the following exponential equations characterizing α and β for wire-form porous sheets were obtained in terms of G_s:

$$\alpha = 39.7 \times A_1 \times 10^8 \left(B \times G_s \times 10^3\right)^{-1.29} \tag{4}$$

and

$$\beta = 35.6 \times A_2 \times 10^5 \left(B \times G_s \times 10^3\right)^{-1.61} \tag{5}$$

or in terms of AFR from the calibration curve of figure 5

$$\alpha = 350 \times A_1 \times 10^8 (AFR)^{-1.29} \tag{6}$$

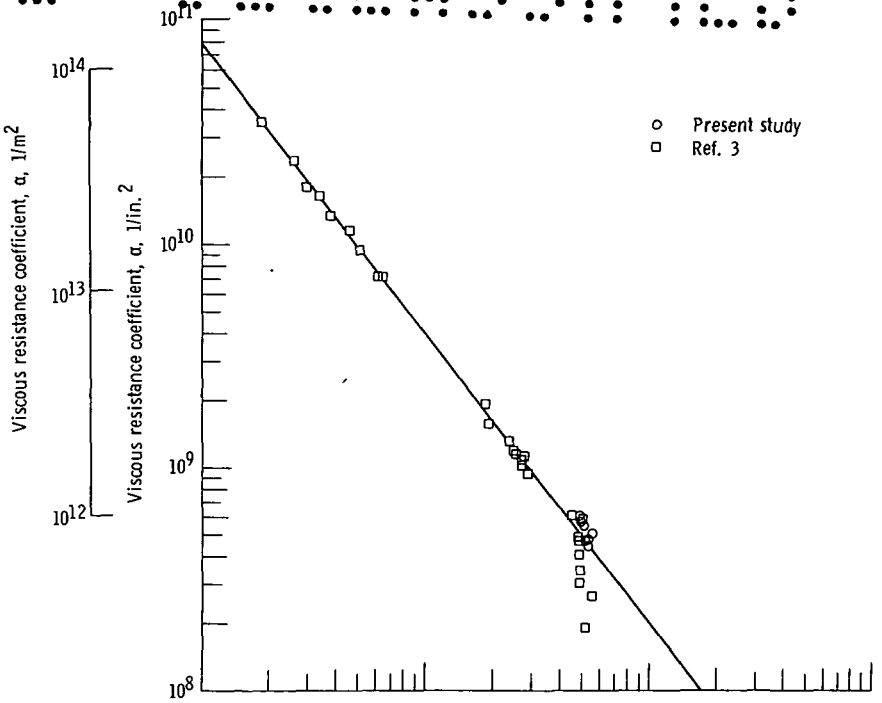

(a) Viscous resistance coefficient correlation.

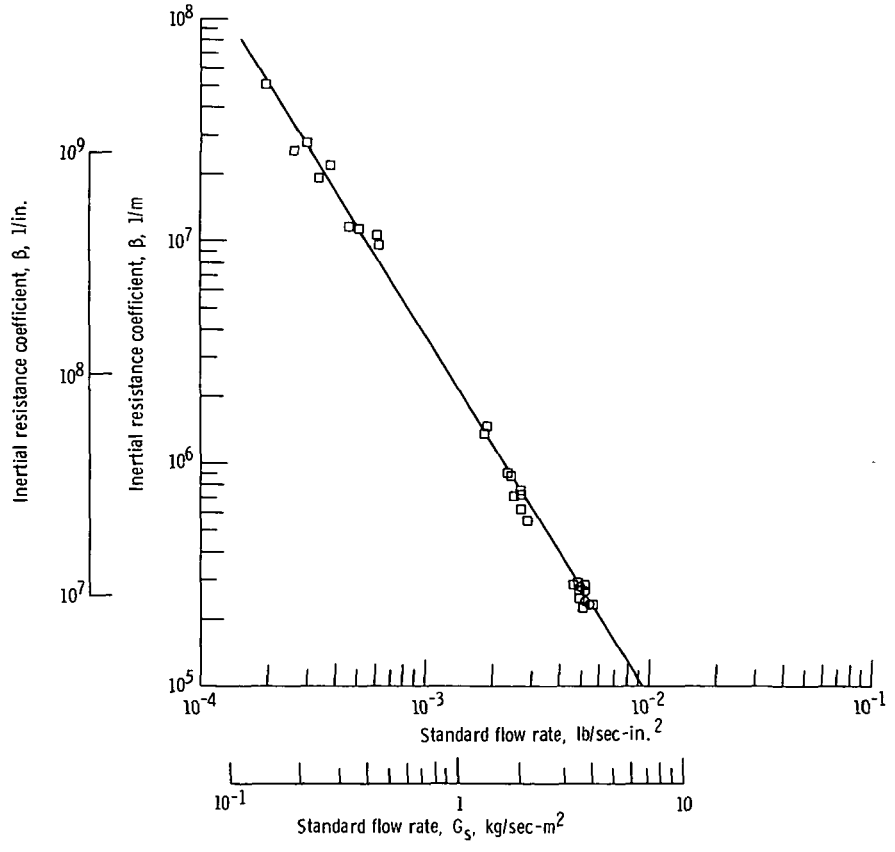

(b) Inertial resistance coefficient correlation.

Figure 6. - Wire-form porous sheet flow data correlation as function of G_s.

and

$$\beta = 540 \times A_2 \times 10^5 (AFR)^{-1.61} \tag{7}$$

where constants A_1, A_2, and B are given in table III.

TABLE III. - CORRELATION CONSTANTS

Constants	Equation where used	Values	
		English units	MKS units
A_1	(4), (6), (8)	1	1550
A_2	(5), (7), (9)	1	39.4
B	(4), (5)	1	703
C	(8), (9)	.096	.00244

Laminate-Form Material Flow Correlation

In figure 7 the flow characteristics, α and β, of 13 different laminate-form porous configurations are correlated against geometrical parameters which are functions of the hydraulic diameter at the minimum internal constriction and the external hole spacing. The data and, therefore, the correlations are only applicable for a standard internal grid pattern which is described in reference 3. The α and β values for each configuration were taken from reference 3. The geometrical parameters were $D_h(\sqrt{C/HS})$ for the α correlation (fig. 7(a)) and $D_h(C/HS)$ for the β correlation (fig. 7(b)), where C is also given in table III. With these parameters, linear correlations were obtained on the log-log plots of figure 7 for the range of geometries and the standard internal grid array which were considered. The exponential equations governing α and β for the laminate-form porous sheets are

$$\alpha = 1.7 \times A_1 \times 10^6 \left(D_h \sqrt{C/HS} \times 10^2\right)^{-6.34} \tag{8}$$

and

$$\beta = 0.60 \times A_2 \times 10^5 \left[D_h (C/HS) \times 10^2\right]^{-3.90} \tag{9}$$

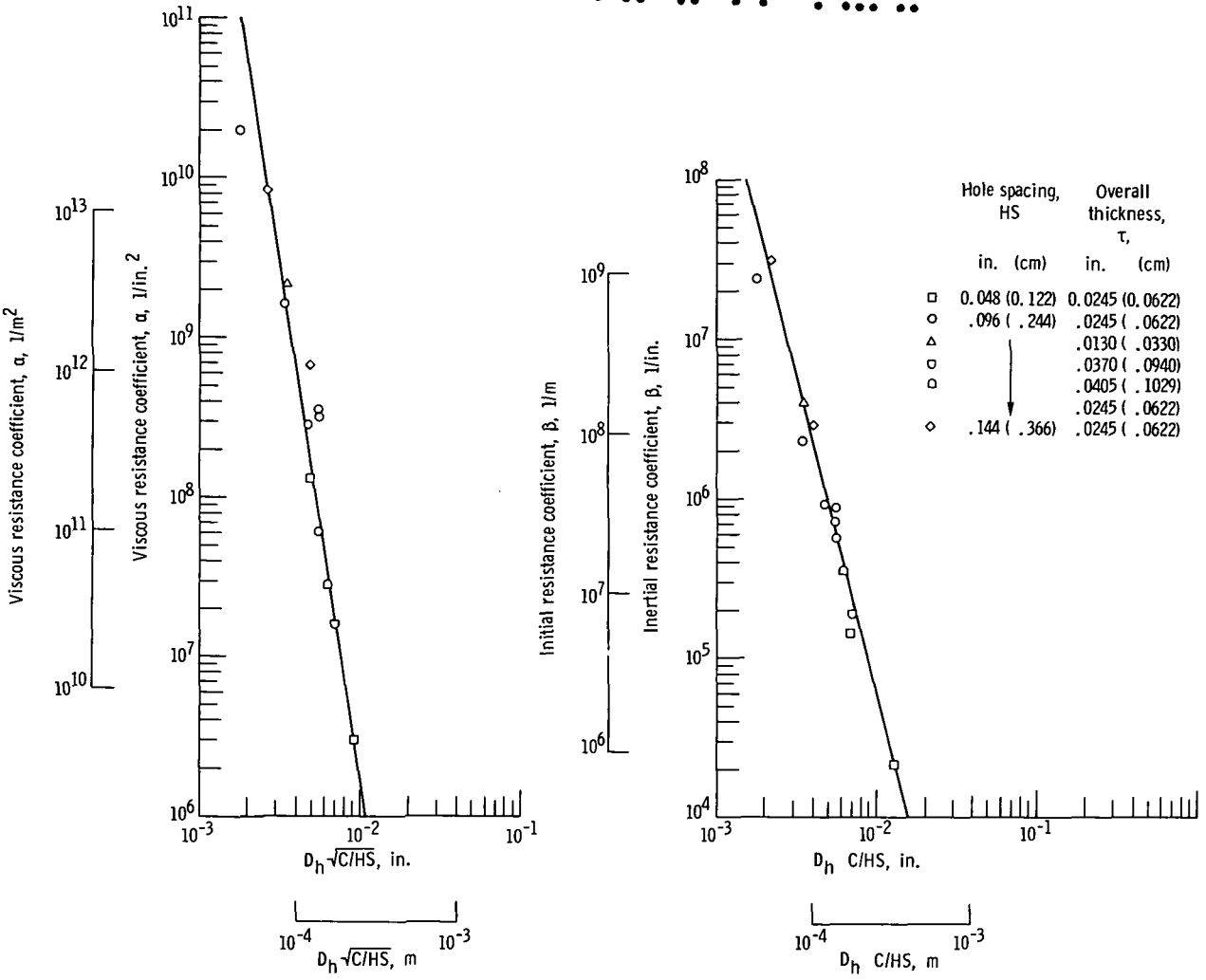

(a) Viscous resistance coefficient correlation.

(b) Inertial resistance coefficient correlation.

Figure 7. - Laminate-form porous sheet flow data correlation as function of hydraulic diameter D_h and hole spacing HS.

Effect of Wire-Form Sheet Curvature

The results of the flow tests on the curved specimens are shown in figure 8. Flow characteristics are nondimensionalized with respect to the values determined for the initial 0.5-inch (1.27-cm) diameter cylinder. The data points represent averages for the three longitudinal locations along each curved surface.

The data scatter in figure 8 can be attributed to measurement inaccuracies arising from the difficulty of having perfect probe contact against curved surfaces with the small radii of curvature used in these tests. The nondimensional flow rate showed a maximum deviation from unity of 7 percent over the range of radii considered although the nondimensional α data scattered a maximum of +20 percent while the nondimensional β

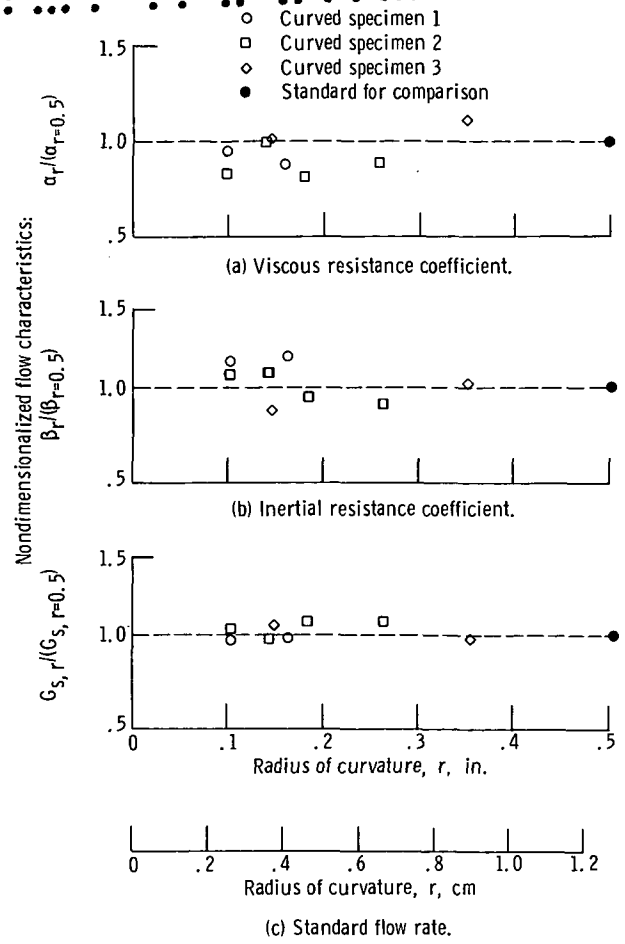

Figure 8. - Effect of wire-form sheet radius of curvature on flow characteristics.

data scattered a maximum of ±16 percent. Since there were no clear trends apparent in the data scatter, it was concluded that the curvature effects on the flow characteristics were minor.

Effect of Hot Airflow

In figure 9 the effects on the α and β flow characteristics of passing 700° to 840° F (644 to 722 K) air through the wire- and laminate-form materials are shown as a function of the air temperature at the test section. The flow characteristics are nondimensionalized with respect to the initial values at room temperature. For purposes of comparison, similar results from reference 3 for standard flow rates from 1.8×10^{-3} to 3.0×10^{-3} pound per second-inch^2 (1.26 to 2.11 kg/sec-m^2) using 300° F (422 K) air are also presented.

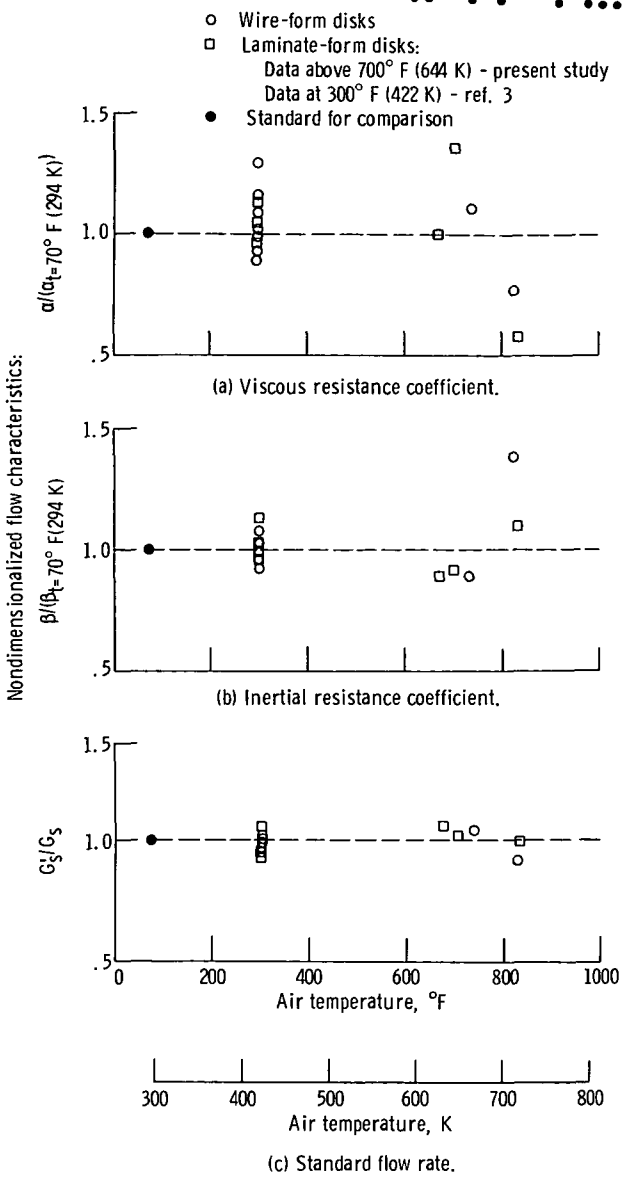

Figure 9. - Effect of air temperature on flow characteristics of wire- and laminate-form disks.

These results show that although there was a large degree of scatter in the α and β coefficients there was relatively little effect on the standard flow rate G'_s over the range of temperatures investigated. This insensitivity of the flow rate to even the rather large scatter in α shown in figure 9(a) for the NASA-Lewis results from laminate-form material was due to the fact that the viscous resistance coefficient would only have a significant effect when the flow rates were extremely small and outside any range of interest for turbine blade transpiration cooling. Another mitigating factor was

that α and β tended to vary in different directions as shown by the NASA-Lewis wire-form results in figures 9(a) and (b), where with 736° F (664 K) air the nondimensional α and β values were 1.11 and 0.89, respectively, and with 825° F (714 K) air the α and β values were 0.77 and 1.38, respectively. Much of the data scatter in figure 9 can be attributed to experimental inaccuracy rather than to any significant trend since the nondimensional data fluctuated on both sides of unity in most instances. It, therefore, appears that the coolant temperature will not have an appreciable effect on the flow rates in the range required for turbine blade cooling in advanced airbreathing engines.

Comparison of Predicted and Measured Flow Rates

Flow rates were calculated for the two wire-form porous disks and two of the three laminate-form porous disks which were tested with elevated temperature air and for the three wire-form curved specimens of 0.1 inch (0.25 cm) radius. The calculation procedure involved first calculating the α and β coefficients from the correlation equations (4) to (7) using the initial G_s or physical parameter value and then applying these to the

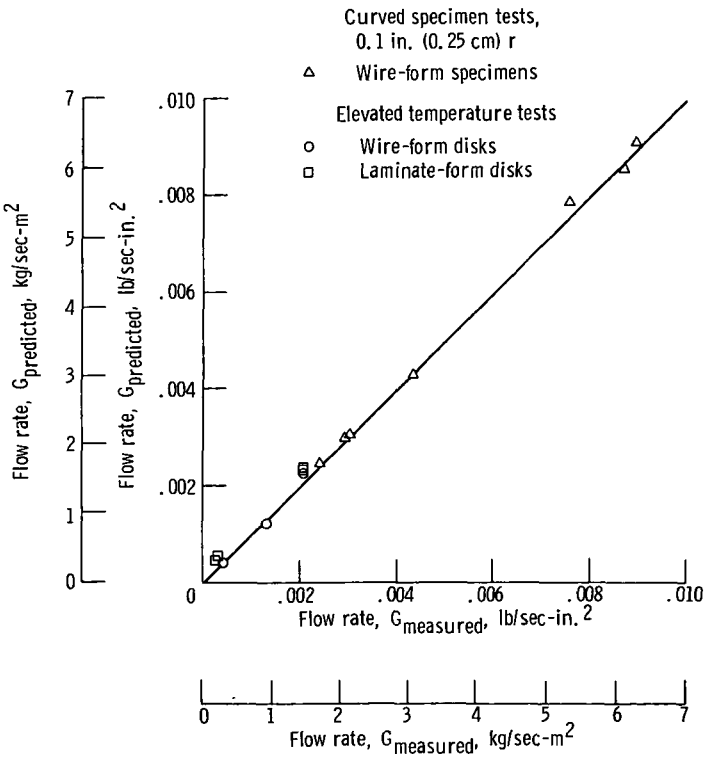

Figure 10. - Comparison of predicted flow rates using correlations and Green equation with measured flow rates.

Green equation (eq. (1)). Unfortunately, there was insufficient information in reference 3 as to the internal geometry of the highest-flow-level laminated disk specimen to compute the hydraulic diameter. The predicted flow rates for the test conditions which gave the maximum and minimum flow for each specimen are compared to the measured flow rates in figure 10. The agreement is fairly good, especially for the wire-form specimens. In the case of the laminate-form specimens, the greater disagreement between predicted and measured flows can be attributed to the fact that the nominal dimensions of the internal constrictions had to be used to obtain the hydraulic diameters since the actual dimensions were not measured. On the other hand, the internal geometries of the laminate-form specimens used for the flow correlations were carefully measured before the laminates were diffusion bonded together. We, therefore, concluded that flow rates can be predicted for both types of porous materials from the Green equation with the α and β values determined from the relations derived herein both for elevated temperature conditions and for curved sheets simulating curvatures in turbine blade airfoils.

CONCLUSIONS

The following conclusions were drawn from this investigation of the flow characteristics of wound wire-form and laminate-form porous materials for transpiration cooling of turbine blades and vanes in advanced airbreathing engines:

1. Flow rates calculated on the basis of the Green equation and the flow characteristic correlations reported herein can be applied with good accuracy to curved portions of airfoils including leading edges and at coolant temperatures up to the maximum temperature investigated of 840° F (722 K).

2. The viscous and inertial resistance coefficients defining the flow through the wire-form material show unique relations with standard flow rate. Flow data in terms of these coefficients can be correlated with standard flow rate (or with the absolute filtration rating as determined from bead tests).

3. The viscous and inertial resistance coefficients of the laminate-form material can be correlated with a combination of the hydraulic diameter at the minimum constriction and the external hole spacing.

4. Flow rates through both wire- and laminate-form materials are relatively insensitive to even large variations or scatter in the viscous and inertial resistance coefficients for the operating conditions applicable to turbine blade transpiration cooling.

Lewis Research Center,
National Aeronautics and Space Administration,
Cleveland, Ohio, June 24, 1970,
720-03.

APPENDIX - SYMBOLS

AFR	absolute filtration rating
D_h	hydraulic diameter
G	airflow rate per unit surface area
G_s	airflow rate per unit area under standard conditions
G'_s	same as G_s but using α and β determined at elevated temperature
g_c	gravitational conversion constant
HS	spacing between holes in square array
K	permeability coefficient
P_1	inlet pressure
P_2	discharge pressure
R	gas constant
T	air temperature
α	viscous resistance coefficient
β	inertial resistance coefficient
μ	viscosity
τ	specimen thickness

Subscripts:

r	with respect to radius r
s	at standard conditions of P_1 = 24.7 psia (17.0 N/cm^2), P_2 = 14.7 psia (10.1 N/cm^2), and 70^o F (294 K)
t	with respect to α or β or both determined at elevated temperature t

[redacted]

REFERENCES

1. Green, Leon, Jr.; and Duwez, Pol: Fluid Flow Through Porous Metals. J. Appl. Mech., vol. 18, no. 1, Mar. 1951, pp. 39-45.

2. Wheeler, H. L., Jr.: Transpiration Cooling in the High Temperature Gas Turbine. Bendix Filter Div., Bendix Corp., Mar. 1964.

3. Anderson, R. D.; and Nealy, D. A.: Evaluation of Laminated Porous Material for High-Temperature Air-Cooled Turbine Blades. Rep. EDR-4968, General Motors Corp. (NASA CR-72281), Jan. 16, 1967.

4. Kaufman, Albert: Analytical Study of Flow Reduction Due to Oxidation of Wire-Form Porous Sheet for Transpiration Cooled Turbine Blades. NASA TN D-5001, 1969.

[redacted]

NASA-Langley, 1970 — 1 E-5748

[redacted]

"The aeronautical and space activities of the United States shall be conducted so as to contribute . . . to the expansion of human knowledge of phenomena in the atmosphere and space. The Administration shall provide for the widest practicable and appropriate dissemination of information concerning its activities and the results thereof."

—NATIONAL AERONAUTICS AND SPACE ACT OF 1958

NASA SCIENTIFIC AND TECHNICAL PUBLICATIONS

TECHNICAL REPORTS: Scientific and technical information considered important, complete, and a lasting contribution to existing knowledge.

TECHNICAL NOTES: Information less broad in scope but nevertheless of importance as a contribution to existing knowledge.

TECHNICAL MEMORANDUMS: Information receiving limited distribution because of preliminary data, security classification, or other reasons.

CONTRACTOR REPORTS: Scientific and technical information generated under a NASA contract or grant and considered an important contribution to existing knowledge.

TECHNICAL TRANSLATIONS: Information published in a foreign language considered to merit NASA distribution in English.

SPECIAL PUBLICATIONS: Information derived from or of value to NASA activities. Publications include conference proceedings, monographs, data compilations, handbooks, sourcebooks, and special bibliographies.

TECHNOLOGY UTILIZATION PUBLICATIONS: Information on technology used by NASA that may be of particular interest in commercial and other non-aerospace applications. Publications include Tech Briefs, Technology Utilization Reports and Notes, and Technology Surveys.

Details on the availability of these publications may be obtained from:

SCIENTIFIC AND TECHNICAL INFORMATION DIVISION

NATIONAL AERONAUTICS AND SPACE ADMINISTRATION

Washington, D.C. 20546

[redacted]